Available online at www.pelagiaresearchlibrary.com

Pelagia Research Library

Advances in Applied Science Research, 2011, 2 (4):259-278

ISSN: 0976-8610
CODEN (USA): AASRFC

Unsteady MHD heat and mass transfer free convection flow of polar fluids past a vertical moving porous plate in a porous medium with heat generation and thermal diffusion

Satya Sagar Saxena[†*] and G. K. Dubey[††]

[†] *Department of Mathematics, Vivekananda College of Technology and Management, Aligarh, U.P., India*
[††]*Department of Mathematics, Agra College, Agra, U.P., India*

ABSTRACT

The unsteady two-dimensional magnetohydrodynamic heat and mass transfer free convection flow of an incompressible, viscous, electrically conducting polar fluid via a porous medium past a semi-infinite vertical porous moving plate in the presence of a transverse magnetic field with thermal diffusion and heat generation is considered. The plate moves with a constant velocity in the longitudinal direction, and the free stream velocity follows an exponentially increasing or decreasing small perturbation law. A uniform magnetic field acts perpendicularly to the porous surface which absorbs the polar fluid with a suction velocity varying with time. The mathematical expressions for velocity, angular velocity, temperature and concentration have been obtained, and the solutions are in terms of exponential functions. Representative results for velocity profiles, temperature profiles and skin friction are obtained both in graphical and tabular form for several values of pertinent parameters which are of physical and engineering interest. The method of solution can be applied for small perturbation approximation. The fluids taken in the study are air (Prandtl number Pr=0.71) and water (Prandtl number Pr=7.0). The numerical results of velocity distribution of polar fluids are compared with the corresponding flow problems for a Newtonian fluid. In the absence of magnetic field, the skin friction decreases in air and increases in water. It is also observed that the effect of increasing values of Prandtl number results in a decreasing skin friction which shows that the skin friction is more in air as compared to that in water.

Key Words: MHD; Free convection; Porous medium; Heat and Mass transfer; Thermal diffusion.
2000 AMS SUBJECT CLASSIFICATION: *76R10, 76R50, 76S05, 76W05*

INTRODUCTION

The study of flow and heat transfer for an electrically conducting polar fluid past a porous plate under the influence of a magnetic field has attracted the interest of many investigators in view of its applications in many engineering problems such as magnetohydrodynamic (MHD) generator,

plasma studies, nuclear reactors, oil exploration, geothermal energy extractions and the boundary layer control in the field of aerodynamics [1]. Also, free convection flows are of great interest in a number of industrial applications such as fiber and granular insulation, geothermal etc. Magnetohydrodynamic has attracted the attention of a large number of scholars due to its diverse applications. In astrophysics and geophysics, it is applied to study the stellar and solar structures, interstellar matter, radio propagation through the ionosphere etc. In engineering, it finds its application in MHD pumps, MHD bearings etc.

Convection in porous media has applications in geothermal energy recovery, oil extraction, thermal energy storage and flow through filtering devices, Nield and Bejan [2]. From technological point of view, MHD free convection flows have significant applications in the field of stellar and planetary magnetosphere, aeronautics, chemical engineering and electronics on account of their varied importance, these flows have been studied by several authors notable amongst them are Shercliff [3], Ferraro and Plumpton [4] and Cramer [5]. Also, many transport processes exist in industries and technology where the transfer of heat and mass occurs simultaneously as a result of thermal diffusion and diffusion of chemical species. In addition, polar fluids are fluids with microstructure belonging to a class of fluids with non-symmetrical stress tensor. Physically, they represent fluids consisting of randomly oriented particles suspended in a viscous medium [6-11, 26, 28]. A great number of Darcian porous MHD studies have been carried out examining the effects of magnetic field on hydrodynamic flow without heat transfer in various configurations, e.g., in channels and past plates and wedges, etc. [12 - 14].

Gribben [15] considered the MHD boundary layer flow over a semi-infinite plate with an aligned magnetic field in the presence of a pressure gradient. He has obtained solutions for large and small magnetic Prandtl numbers using the method of matched asymptotic expansion. Takhar and Ram [16] studied the effects of Hall currents on hydromagnetic free convection boundary layer flow via a porous medium past a plate, using harmonic analysis. Takhar and Ram [17] also studied the MHD free porous convection heat transfer of water at 4^0C through a porous medium. Soundalgekar [18] obtained approximate solutions for the two-dimensional flow of an incompressible, viscous fluid past an infinite porous vertical plate with constant suction velocity normal to the plate, the difference between the temperature of the plate and the free stream is moderately large causing the free convection currents.

Raptis and Kafousias [19] studied the influence of a magnetic field upon the steady free convection flow through a porous medium bounded by an infinite vertical plate with a constant suction velocity, and when the plate temperature is also constant. Raptis [20] studied mathematically the case of time-varying two-dimensional natural convective heat transfer of an incompressible, electrically conducting viscous fluid via a highly porous medium bounded by an infinite vertical porous plate.

A study on MHD heat and mass transfer free convection flow along a vertical stretching sheet in the presence of magnetic field with heat generation was carried out by Samad and Mohebujjaman [23]. Saravana et al. [24] studied the mass transfer effects on MHD viscous flow past an impulsively started infinite vertical plate with constant mass flux. Singh [25] analyzed the MHD free convection and mass transfer flow with heat source and thermal diffusion. The

paper deals with the study of free convection and mass transfer flow of an incompressible, viscous and electrically conducting fluid past a continuously moving infinite vertical plate in the presence of large suction and under the influence of uniform magnetic field considering heat source and thermal diffusion. Kim [27] considered the unsteady magnetohydrodynamic convective heat transfer past a semi-infinite vertical porous moving plate with variable suction.

However, most of the previous works assume that the plate is at rest. In the present work, we consider the case of a semi-infinite moving porous plate with a constant velocity in the longitudinal direction when the magnetic field is imposed transversely to the plate. We also consider the free stream to consist of a mean velocity and temperature with a superimposed exponentially variation with time. In view of the applications of free convective phenomenon, heat source and thermal diffusion, in the present work it is proposed to study the unsteady two-dimensional MHD free convective heat and mass transfer of polar fluids past a semi-infinite vertical moving porous plate via a porous medium taking into account the combined effect of heat source and thermal diffusion. The aim of this paper is to make a numerical calculation, on convective heat and mass transfer flow which have been of interest to the engineering community and to the investigators dealing with the problem in geophysics, astrophysics, plasma studies, nuclear reactors etc. From the technical point of view, free convective flow past an infinite or semi-infinite vertical plate is always important for many practical applications.

In general, the study of Darcian porous MHD is very complicated. It is necessary to consider in detail the distribution of velocity and temperature distributions across the boundary layer. Representative results for the velocity, angular velocity and temperature profiles are displayed graphically showing the effect of several governing parameters entering into the problem. Also, we have prepared a table of the values of skin friction displaying the effects of various material parameters. To the best of our knowledge this problem has not been studied before and the results reported here are new.

NOMENCLATURE

A	:	suction velocity parameter
B_0	:	magnetic flux density
C	:	concentration of the fluid within the boundary layer
C_p	:	specific heat at constant pressure
G_r	:	Grashof number
G_c	:	Modified Grashof number
g	:	acceleration due to gravity
K	:	permeability parameter
k	:	thermal conductivity
M	:	Magnetic field parameter
N	:	dimensionless material parameter
Nu	:	Nusselt number
n	:	dimensionless exponential index
P_r	:	Prandtl number
T	:	temperature
t	:	dimensionless time
U_0	:	scale of free stream velocity

u, v : component of velocities along and perpendicular to the plate, respectively
V_0 : scale of suction velocity
x, y : distances along and perpendicular to the plate, respectively

GREEK SYMBOLS

β : dimensionless viscosity ratio
β_f : coefficient of volumetric expansion of the working fluid
β_c : coefficient of concentration expansion
γ : spin-gradient viscosity
ε : scalar constant (<< 1)
σ : electrical conductivity
ρ : fluid density
Λ : coefficient of gyro-viscosity
μ : fluid dynamic viscosity
υ : fluid kinematic viscosity
υ_r : fluid kinematic rotational viscosity
θ : dimensionless temperature
τ : skin friction
ω : angular velocity vector
ϕ : dimensionless concentration

SUPERSCRIPTS

' : differentiation with respect to y
* : dimensional properties

SUBSCRIPTS

p : plate
w : wall condition
∞ : free stream condition

FORMULATION

We consider the two-dimensional unsteady free convective heat and mass transfer flow of a laminar, incompressible fluid past a semi-infinite vertical porous moving plate embedded in a porous medium and subjected to a transverse magnetic field in the presence of a pressure gradient. The physical model and geometrical coordinates are shown in Fig. 1. It is assumed that there is no applied voltage which implies the absence of an electric field. The transversely applied magnetic field and magnetic Reynolds number are very small and hence the induced magnetic field is negligible [21]. Viscous and Darcy's resistance terms are taken into account with constant permeability of the porous medium. The MHD term is derived from an order-of-magnitude analysis of the full Navier-Stokes equations. It is assumed here that the hole size of the porous plate is significantly larger than a characteristic microscopic length scale of the porous medium. We regard the porous medium as an assemblage of small identical spherical particles fixed in space, following Yamamoto and Iwamura [22]. Due to the semi-infinite plane surface assumption, furthermore, the flow variables are functions of y^* and t^* only.

Under these conditions, the governing equations, i.e. the mass, momentum, energy conservation and diffusion equations can be written in a Cartesian frame of reference, as:

continuity: $$\frac{\partial v^*}{\partial y^*} = 0 \qquad (1)$$

linear momentum:

$$\frac{\partial u^*}{\partial t^*} + v^* \frac{\partial u^*}{\partial y^*} = -\frac{1}{\rho}\frac{\partial p^*}{\partial x^*} + (\upsilon + \upsilon_r)\frac{\partial^2 u^*}{\partial y^{*2}} + g\beta_f (T - T_\infty) + g\beta_c (C - C_\infty) - \upsilon \frac{u^*}{K^*} - \frac{\sigma}{\rho} B_0^2 u^* + 2\upsilon_r \frac{\partial \omega^*}{\partial y^*} \qquad (2)$$

angular momentum: $$\rho\, j^* \left(\frac{\partial \omega^*}{\partial t^*} + v^* \frac{\partial \omega^*}{\partial y^*} \right) = \gamma \frac{\partial^2 \omega^*}{\partial y^{*2}} \qquad (3)$$

energy: $$\frac{\partial T}{\partial t^*} + v^* \frac{\partial T}{\partial y^*} = \frac{k}{\rho C_p}\frac{\partial^2 T}{\partial y^{*2}} + \frac{S^*}{\rho C_p}(T - T_\infty) \qquad (4)$$

diffusion: $$\frac{\partial C}{\partial t^*} + v^* \frac{\partial C}{\partial y^*} = D\frac{\partial^2 C}{\partial y^{*2}} + D_1 \frac{\partial^2 T}{\partial y^{*2}} \qquad (5)$$

where x^* and y^* are the dimensional distances longitudinal and perpendicular to the plate, respectively, u^* and v^* the components of dimensional velocities along the x^* and y^* directions, respectively, K^* the permeability of the porous medium, σ the electrical conductivity of the fluid, B_0 the magnetic induction, j^* the micro-inertia density, ω^* the component of the angular velocity vector normal to the xy-plane, S^* is the coefficient of heat source, D is the chemical molecular diffusivity and D_1 is the thermal diffusivity.

The third term on the RHS of the momentum equation (2) denotes buoyancy effects, the fourth is the bulk matrix linear resistance, i.e., Darcy term, the fifth is the MHD term. Also, Darcy dissipation term is neglected because it is of the same order-of-magnitude as the viscous dissipation term. It is assumed that the porous plate moves with constant velocity (u_p^*) in the longitudinal direction, and the free stream velocity (U_∞^*) follows an exponentially increasing or decreasing small perturbation law. We also assume that the plate temperature (T) and suction velocity (v^*) vary exponentially with time.

Under the above assumptions, the appropriate boundary conditions for the velocity, temperature and concentration fields are

$$u^* = u_p^*, T = T_w + \varepsilon(T_w - T_\infty)e^{n^* t^*}, C = C_w + \varepsilon(C_w - C_\infty)e^{n^* t^*}, \frac{\partial \omega^*}{\partial y^*} = -\frac{\partial^2 u^*}{\partial y^{*2}} \quad \text{at } y^* = 0 \qquad (6)$$

$$u^* \to U_\infty^* = U_0(1 + \varepsilon e^{n^* t^*}), T \to T_\infty, C \to C_\infty, \omega^* \to 0 \quad \text{as } y^* \to \infty \qquad (7)$$

in which n^* is a scalar constant, and U_0 is a scale of free stream velocity.

From the continuity equation (1), it is clear that the suction velocity normal to the plate is a function of time only and we shall take it in the form:

$$v^* = -V_0(1+\varepsilon A e^{n^* t^*}) \tag{8}$$

where A is a real positive constant, ε and εA small less than unity and V_0 is a scale of suction velocity which has non-zero positive constant. Outside the boundary layer, equation (2) gives

$$-\frac{1}{\rho}\frac{dp^*}{dx^*} = \frac{dU_\infty^*}{dt^*} + \frac{\upsilon}{K^*}U_\infty^* + \frac{\sigma}{\rho}B_0^2 U_\infty^* \tag{9}$$

We now introduce the dimensionless variables, as follows:

$$\left.\begin{aligned}
&u = \frac{u^*}{U_0}, v = \frac{v^*}{V_0}, y = \frac{V_0 y^*}{\upsilon}, U_\infty = \frac{U_\infty^*}{U_0}, U_p = \frac{u_p^*}{U_0}, \omega = \frac{\upsilon}{U_0 V_0}\omega^*, t = \frac{t^* V_0^2}{\upsilon},\\
&\theta = \frac{T-T_\infty}{T_w - T_\infty}, \quad \phi = \frac{C-C_\infty}{C_w - C_\infty}, n = \frac{n^*\upsilon}{V_0^2}, K = \frac{K^* V_0^2}{\upsilon^2}, j = \frac{V_0^2}{\upsilon^2} j^*,\\
&S_C = \frac{\upsilon}{D} \text{ is the Schmidt number, } P_r = \frac{\upsilon\rho C_p}{k} = \frac{\mu C_p}{k} \text{ is the Prandtl number,}\\
&M = \frac{\sigma B_0^2 \upsilon}{\rho V_0^2} \text{ is the magnetic field parameter, } G_r = \frac{\upsilon\beta_f g(T_w - T_\infty)}{U_0 V_0^2} \text{ is the Grashof number,}\\
&G_c = \frac{\upsilon\beta_c g(C_w - C_\infty)}{U_0 V_0^2} \text{ is the modified Grashof number,}\\
&A_1 = \frac{D_1}{\upsilon}\left(\frac{T_w - T_\infty}{C_w - C_\infty}\right) \text{ is thermal diffusion parameter,}\\
&S = \frac{S^*\upsilon}{\rho C_p V_0^2} \text{ is the heat source parameter}
\end{aligned}\right\} \tag{10}$$

Furthermore, the spin-gradient viscosity γ which gives some relationship between the coefficients of viscosity and micro-inertia, is defined as

$$\gamma = \left(\mu + \frac{\Lambda}{2}\right) j^* = \mu j^* \left(1 + \frac{1}{2}\beta\right) \tag{11}$$

where β denotes the dimensionless viscosity ratio, defined as follows:

$$\beta = \frac{\Lambda}{\mu} \tag{12}$$

in which Λ is the coefficient of gyro-viscosity (or vortex viscosity).

In view of equations (8)-(12), the governing equations (2)-(5) reduce to the following non-dimensional form:

$$\frac{\partial u}{\partial t} - (1+\varepsilon A e^{nt})\frac{\partial u}{\partial y} = \frac{dU_\infty}{dt} + (1+\beta)\frac{\partial^2 u}{\partial y^2} + G_r\theta + G_c\phi + N(U_\infty - u) + 2\beta\frac{\partial \omega}{\partial y} \tag{13}$$

$$\frac{\partial \omega}{\partial t} - (1+\varepsilon A e^{nt})\frac{\partial \omega}{\partial y} = \frac{1}{\eta}\frac{\partial^2 \omega}{\partial y^2} \tag{14}$$

$$\frac{\partial \theta}{\partial t} - (1+\varepsilon A e^{nt})\frac{\partial \theta}{\partial y} = \frac{1}{P_r}\frac{\partial^2 \theta}{\partial y^2} + S\theta \tag{15}$$

$$\frac{\partial \phi}{\partial t} - (1+\varepsilon A e^{nt})\frac{\partial \phi}{\partial y} = \frac{1}{S_c}\frac{\partial^2 \phi}{\partial y^2} + A_1\frac{\partial^2 \theta}{\partial y^2} \tag{16}$$

where

$$N = \left(M + \frac{1}{K}\right), \quad \eta = \frac{\mu j^*}{\gamma} = \frac{2}{2+\beta}$$

The boundary conditions (6) and (7) are then given by the following dimensionless form:

$$u = U_p,\ \theta = 1+\varepsilon e^{nt},\ \phi = 1+\varepsilon e^{nt},\ \frac{\partial \omega}{\partial y} = -\frac{\partial^2 u}{\partial y^2} \qquad \text{at } y = 0 \tag{17}$$

$$u \to U_\infty,\ \theta \to 0,\ \phi \to 0,\ \omega \to 0 \qquad \text{as } y \to \infty \tag{18}$$

where U_p is the plate moving velocity.

SOLUTION

In order to reduce the above system of partial differential equations to a system of ordinary differential equations in dimensionless form, we may represent the linear and angular velocities, temperature and concentration as

$$u = u_0(y) + \varepsilon e^{nt} u_1(y) + O(\varepsilon^2) + \cdots\cdots \tag{19}$$

$$\omega = \omega_0(y) + \varepsilon e^{nt} \omega_1(y) + O(\varepsilon^2) + \cdots\cdots \tag{20}$$

$$\theta = \theta_0(y) + \varepsilon e^{nt} \theta_1(y) + O(\varepsilon^2) + \cdots\cdots \tag{21}$$

$$\phi = \phi_0(y) + \varepsilon e^{nt} \phi_1(y) + O(\varepsilon^2) + \cdots\cdots \tag{22}$$

Substituting equations (19)-(22) in equations (13)-(16) and equating the harmonic and non-harmonic terms, neglecting the coefficient of $O(\varepsilon^2)$, we get the following pairs of equations for $(u_0, \omega_0, \theta_0, \phi_0)$ and $(u_1, \omega_1, \theta_1, \phi_1)$.

$$(1+\beta)u_0'' + u_0' - N u_0 = -N - G_r\theta_0 - G_c\phi_0 - 2\beta\omega_0', \tag{23}$$

$$(1+\beta)u_1'' + u_1' - (N+n)u_1 = -(N+n) - Au_0' - G_r\theta_1 - G_c\phi_1 - 2\beta\omega_1', \tag{24}$$

$$\omega_0'' + \eta\omega_0' = 0, \tag{25}$$

$$\omega_1'' + \eta\omega_1' - n\eta\omega_1 = -A\eta\omega_0', \tag{26}$$

$$\theta_0'' + P_r\theta_0' + SP_r\,\theta_0 = 0 \tag{27}$$

$$\theta_1'' + P_r\theta_1' - P_r(n-S)\theta_1 = -AP_r\theta_0' \tag{28}$$

$$\phi_0'' + S_c\phi_0' = -A_1 S_c\,\theta_0'' \tag{29}$$

$$\phi_1'' + S_c\phi_1' - nS_c\phi_1 = -AS_c\phi_0' - A_1S_c\,\theta_1'' \tag{30}$$

Here primes denote differentiation with respect to *y*. The corresponding boundary conditions can be written as:

$$u_0 = U_p,\ u_1 = 0,\ \omega_0' = -u_0'',\ \omega_1' = -u_1'',\quad \theta_0 = 1,\ \theta_1 = 1,\ \phi_0 = 1,\ \phi_1 = 1 \quad \text{at } y = 0 \tag{31}$$

$$u_0 = 1,\ u_1 = 1,\ \omega_0 \to 0,\ \omega_1 \to 0,\ \theta_0 \to 0,\ \theta_1 \to 0,\ \phi_0 \to 0,\ \phi_1 \to 0 \quad \text{as } y \to \infty \tag{32}$$

The solutions of equations (23)-(30) satisfying boundary conditions (31) and (32) are given by

$$u_0(y) = 1 + a_1e^{-h_2y} + a_2e^{-h_5y} + a_3e^{-\eta y} - (1+a_4)a_{10}e^{-S_cy} + a_{11}a_4e^{-h_5y}, \tag{33}$$

$$u_1(y) = 1 + b_1e^{-h_1y} + b_2e^{-h_2y} + b_3e^{-h_3y} + b_4e^{-h_4y} + b_5e^{-h_5y} + b_6e^{-\eta y} + b_7e^{-h_7y} + b_8e^{-S_cy}, \tag{34}$$

$$\omega_0(y) = c_1e^{-\eta y}, \tag{35}$$

$$\omega_1(y) = c_2e^{-h_1y} - \frac{A\eta}{n}c_1e^{-\eta y}, \tag{36}$$

$$\theta_0(y) = e^{-h_5y}, \tag{37}$$

$$\theta_1(y) = e^{-h_4y} + \frac{A}{h_6}P_r(e^{-h_4y} - e^{-h_5y}), \tag{38}$$

$$\phi_0(y) = e^{-S_cy} + a_4(e^{-S_cy} - e^{-h_5y}), \tag{39}$$

$$\phi_1(y) = k_3e^{-h_7y} + a_7e^{-S_cy} + a_8e^{-h_5y} + a_9e^{-h_4y}, \tag{40}$$

where

$$h_1 = \frac{\eta}{2}\left(1 + \sqrt{1 + \frac{4n}{\eta}}\right),\quad h_2 = \frac{1}{2(1+\beta)}\left[1 + \sqrt{1 + 4N(1+\beta)}\right],\quad h_3 = \frac{1}{2(1+\beta)}\left[1 + \sqrt{1 + 4(N+n)(1+\beta)}\right],$$

$$h_4 = \frac{P_r}{2}\left(1 + \sqrt{1 + \frac{4(n-S)}{P_r}}\right),\quad h_5 = \frac{P_r}{2}\left[1 + \sqrt{1 - \frac{4S}{P_r}}\right],\quad h_6 = -\frac{h_5^2 - P_rh_5 - P_r(n-S)}{h_5},$$

$$h_7 = \frac{S_c}{2}\left(1 + \sqrt{1 + \frac{4n}{S_c}}\right),\quad a_1 = U_p - 1 - a_2 - a_3 + (1+a_4)a_{10} - a_{11}a_4,\quad a_2 = \frac{-G_r}{(1+\beta)h_5^2 - h_5 - N},$$

$$a_3 = \frac{2\beta\eta}{(1+\beta)\eta^2 - \eta - N}c_1,\quad a_4 = \frac{A_1S_ch_5}{h_5 - S_c},\quad a_5 = \frac{AS_ch_5}{h_6}(A_1P_rh_5 - a_4h_6),\quad a_6 = \frac{A_1S_ch_4^2}{h_6}(h_6 + AP_r),$$

$$a_7 = -\frac{AS_c}{n}(1+a_4),\quad a_8 = \frac{a_5}{h_5^2 - S_ch_5 - nS_c},\quad a_9 = -\frac{a_6}{h_4^2 - S_ch_4 - nS_c},\quad a_{10} = \frac{G_c}{(1+\beta)S_c^2 - S_c - N},$$

$$a_{11} = \frac{G_c}{(1+\beta)h_5^2 - h_5 - N},\quad b_1 = \frac{2\beta h_1}{(1+\beta)h_1^2 - h_1 - (N+n)}c_2,\quad b_2 = -\frac{Ah_2}{n}a_1,$$

$$b_3 = \frac{2\beta h_1}{(1+3\beta)h_1^2 - h_1 - 2\beta h_3^2 - (N+n)}\left[\frac{(1+3\beta)h_1^2 - h_1 - (N+n)}{2\beta h_1}k_2 + \frac{k_1}{h_1}\right],$$

$$b_4 = -\left[G_r\left(1+\frac{AP_r}{h_6}\right)+G_c a_9\right]\frac{1}{(1+\beta)h_4^2 - h_4 - (N+n)},$$

$$b_5 = \left[Ah_5(a_2 + a_{11}a_4)+\left(\frac{G_r AP_r}{h_6}\right)-G_c a_8\right]\frac{1}{(1+\beta)h_5^2 - h_5 - (N+n)}, \quad b_6 = \frac{A\eta a_3 - \left\{\frac{2\beta A\eta^2}{n}\right\}c_1}{(1+\beta)\eta^2 - \eta - (N+n)},$$

$$b_7 = \frac{-G_c k_3}{(1+\beta)h_7^2 - h_7 - (N+n)}, \; b_8 = -\left[A(1+a_4)a_{10}S_c + G_c a_7\right]\frac{1}{(1+\beta)S_c^2 - S_c - (N+n)},$$

$$c_1 = \frac{(1+\beta)\eta - 1 - (N/\eta)}{(1-\beta)\eta^2 - \eta - N + 2\beta h_2^2}\left[(U_p - 1)h_2^2 + (h_5^2 - h_2^2)(a_2 + a_{11}a_4) + (h_2^2 - S_c^2)(1+a_4)a_{10}\right],$$

$$c_2 = -\frac{1}{h_1}\left[k_1 + b_1 h_1^2 + b_3 h_3^2\right], \quad k_1 = -\frac{A\eta^2}{n}c_1 + b_2 h_2^2 + b_4 h_4^2 + b_5 h_5^2 + b_6\eta^2 + b_7 h_7^2 + b_8 S_c^2,$$

$$k_2 = -(1 + b_2 + b_4 + b_5 + b_6 + b_7 + b_8), \quad k_3 = 1 - a_7 - a_8 - a_9$$

By virtue of equations (19)-(22), we obtain the velocity, angular velocity, temperature and concentration, as follows:

$$u(y,t) = 1 + a_1 e^{-h_2 y} + a_2 e^{-h_5 y} + a_3 e^{-\eta y} - (1+a_4)a_{10}e^{-S_c y} + a_{11}a_4 e^{-h_5 y}$$

$$+\varepsilon e^{nt}\left[1 + b_1 e^{-h_1 y} + b_2 e^{-h_2 y} + b_3 e^{-h_3 y} + b_4 e^{-h_4 y} + b_5 e^{-h_5 y} + b_6 e^{-\eta y} + b_7 e^{-h_7 y} + b_8 e^{-S_c y}\right] \quad (41)$$

$$\omega(y,t) = c_1 e^{-\eta y} + \varepsilon e^{nt}\left[c_2 e^{-h_1 y} - \frac{A\eta}{n}c_1 e^{-\eta y}\right] \quad (42)$$

$$\theta(y,t) = e^{-h_5 y} + \varepsilon e^{nt}\left[e^{-h_4 y} + \frac{A}{h_6}P_r(e^{-h_4 y} - e^{-h_5 y})\right] \quad (43)$$

$$\phi(y,t) = e^{-S_c y} + a_4(e^{-S_c y} - e^{-h_5 y}) + \varepsilon e^{nt}\left[k_3 e^{-h_7 y} + a_7 e^{-S_c y} + a_8 e^{-h_5 y} + a_9 e^{-h_4 y}\right] \quad (44)$$

Given the velocity field in the boundary layer, we can now calculate the skin friction at the wall of the plate, which is given by

$$\tau_w = \frac{\tau_w^*}{\rho U_0 V_0} = \left(\frac{\partial u}{\partial y}\right)_{y=0}$$
$$= -a_1 h_2 - a_2 h_5 - a_3 \eta + (1+a_4) a_{10} S_c - a_{11} a_4 h_5$$
$$- \varepsilon e^{nt} \left[b_1 h_1 + b_2 h_2 + b_3 h_3 + b_4 h_4 + b_5 h_5 + b_6 \eta + b_7 h_7 + b_8 S_c \right] \quad (45)$$

We can also calculate the heat transfer coefficient in terms of the Nusselt number, as follows:

$$Nu = x \frac{\left(\partial T \big/ \partial y^*\right)_w}{T_w - T_\infty} , \quad (46)$$

$$Nu \, \mathrm{Re}_x^{-1} = \left(\frac{\partial \theta}{\partial y}\right)_{y=0} = -h_5 + \varepsilon e^{nt} \left[\frac{AP_r}{h_6} h_5 - h_4 \left(1 + \frac{AP_r}{h_6}\right) \right] \quad (47)$$

where $\mathrm{Re}_x = V_0 x \big/ \upsilon$ is the Reynolds number.

RESULTS AND DISCUSSION

In the preceding sections, we have obtained the mathematical expressions for u, ω, θ and ϕ. The solutions are in terms of exponential functions. In this section, the numerical computations have been made for the velocity, angular velocity and temperature for various values of flow and material parameters n, t, A, ε, M, K, G_r, G_c, U_p, A_1, S_c, S which are listed in the figure captions. Also, we have obtained the computed values of skin friction for different values of material parameters. The boundary condition for $y \to \infty$ is replaced by identical ones at y_{max} which is a sufficiently large value of y where the velocity profile u approaches the relevant free stream velocity. Generally, we choose $y_{max} = 6$ and a step size $\Delta y = 0.001$. The fluids taken in this study are air ($P_r = 0.71$) and water ($P_r = 7.0$) and all the graphs are plotted against y.

The general distributions of velocity and temperature profiles of Newtonian fluid across the boundary layer for a stationary porous plate in the case of absence of magnetic field are shown in Fig. 2. It is observed that the velocity and temperature decrease in water compared with air.

The velocity and angular velocity profiles for various values of viscosity ratio β are displayed in Fig. 3. It is observed that the velocity distribution is lower for a Newtonian fluid ($\beta = 0$) with the fixed flow and material parameters, as compared with a polar fluid when the viscosity ratio is less than 0.5. For a Newtonian fluid ($\beta = 0$), the velocity graph in water is lower than the respective velocity graph in air while this situation is reverse in case of angular velocity. When β takes values larger than 0.5, however, the velocity distribution shows a decelerating nature near the porous plate. In addition, the angular velocity distributions do not show consistent variations with increment of β.

For the case of a stationary porous plate, Fig. 4 concerns with the effect of dimensionless exponential index n on the velocity in air and water. It is clear that when approaching $n \to 0^+$,

the magnitude of the velocity distribution across the boundary layer increases, and then decays to the relevant free stream velocity. Also, when *n* increases from 0.1 to 0.4, the velocity decreases.

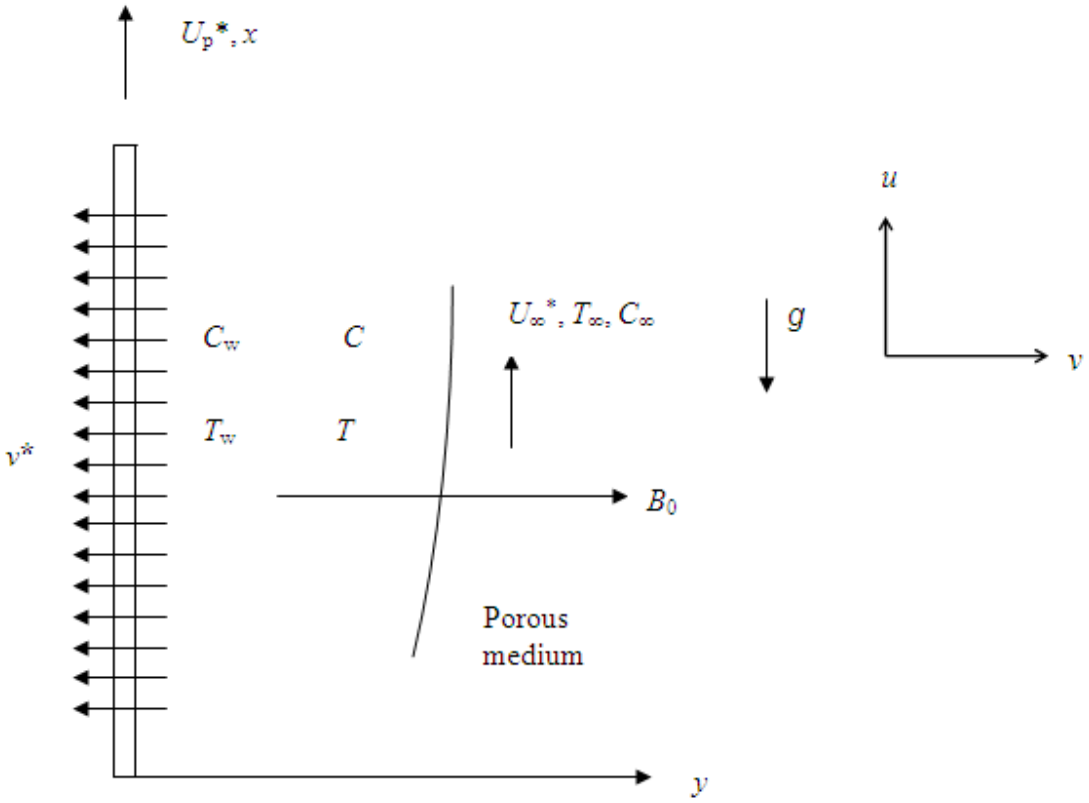

Fig.1. Flow configuration and coordinate system

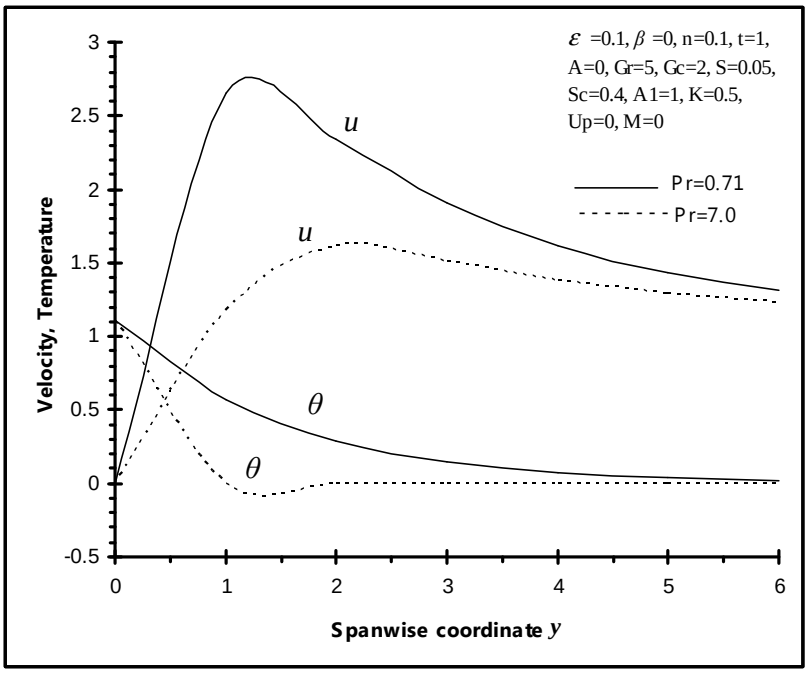

Fig.2. Distribution of velocity and temperature profiles of Newtonian fluid across the boundary layer for a stationary vertical porous plate in air and water in the absence of magnetic field

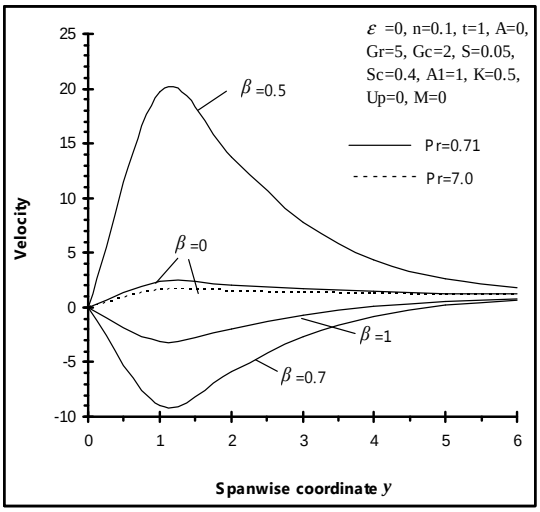

Fig.3 (a)

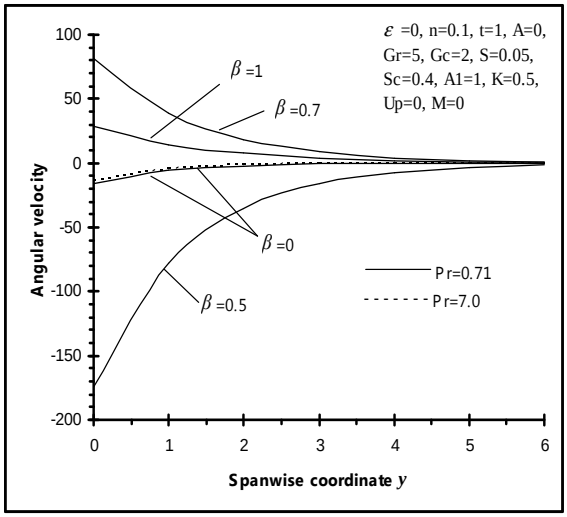

Fig.3 (b)

Fig.3. Velocity and angular velocity profiles against spanwise coordinate *y* for different values of viscosity ratio β

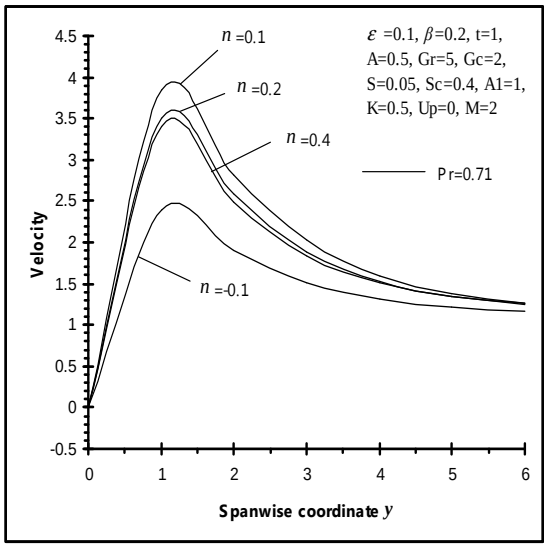

Fig.4 (a)

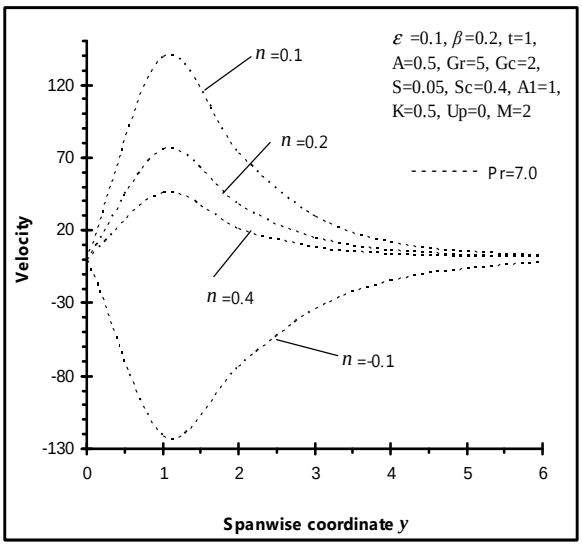

Fig.4 (b)

Fig.4. Velocity profiles against spanwise coordinate *y* for different values of dimensionless exponential index *n*

Fig. 5 displays the velocity and angular velocity profiles across the boundary layer for different values of the plate velocity U_p. The peak value of velocity across the boundary layer decreases near the porous plate as the plate velocity increases. Also, the velocity across the boundary layer increases in water and then decays to the relevant free stream velocity. However, the angular velocity increases as the plate velocity increases. It is also observed that at some fixed value of U_p, the angular velocity graph in air is lower than the respective angular velocity graph in water.

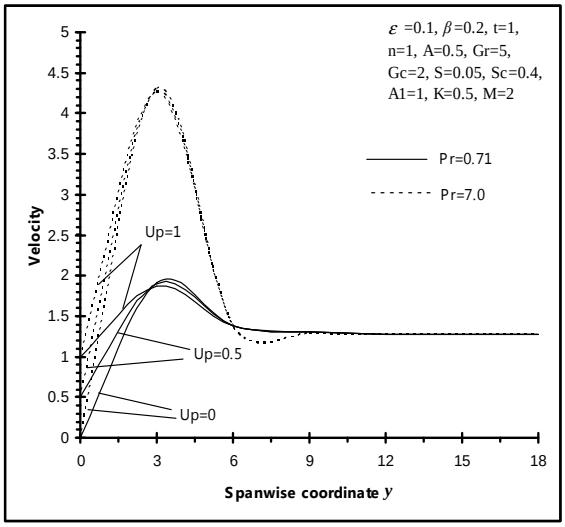

Fig.5 (a)

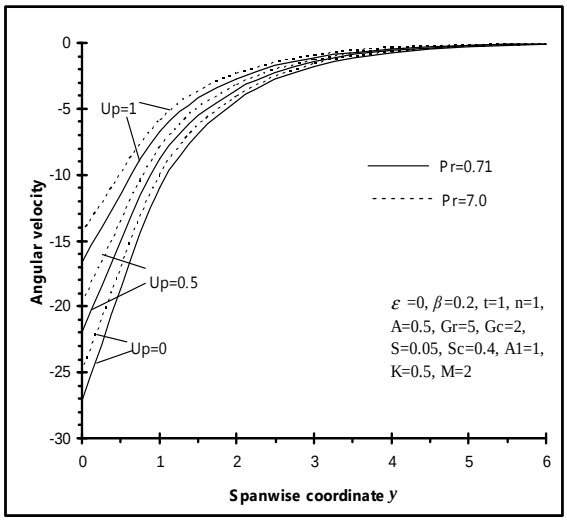

Fig.5 (b)

Fig.5. Velocity and angular velocity profiles against spanwise coordinate *y* for different values of plate moving velocity U_p

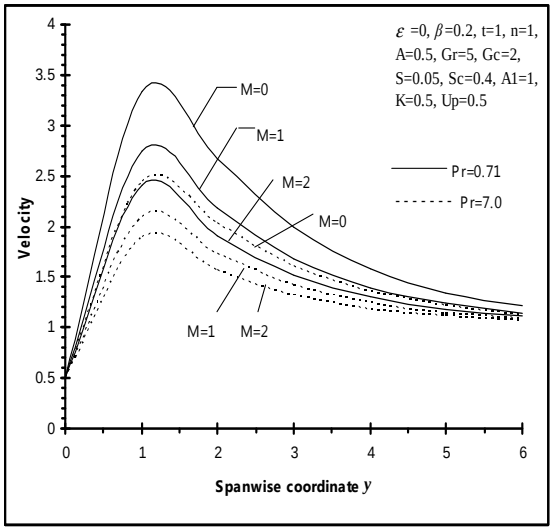

Fig.6 (a)

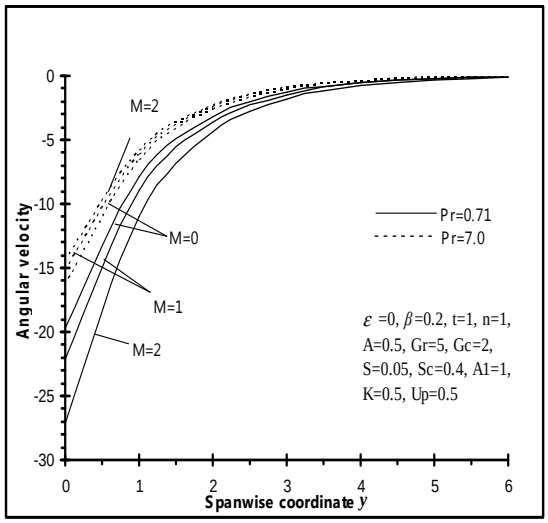

Fig.6 (b)

Fig.6. Velocity and angular velocity profiles against spanwise coordinate *y* for different values of magnetic parameter *M*

Fig. 6 depicts the velocity and angular velocity profiles for different values of the magnetic field parameter *M*. In air and water, it is observed that the velocity decreases with the increasing values of magnetic field parameter which shows that the velocity decreases in the presence of magnetic field, as compared to its absence. This agrees with the expectations, since the magnetic field exerts a retarding force on the free convective flow. Furthermore, it is clear that due to increasing values of *M*, the values of angular velocity on the porous plate are decreased in air and increased in water. It is also observed that for different values of *M*, the angular velocity graphs in air are lower than the respective angular velocity graphs in water.

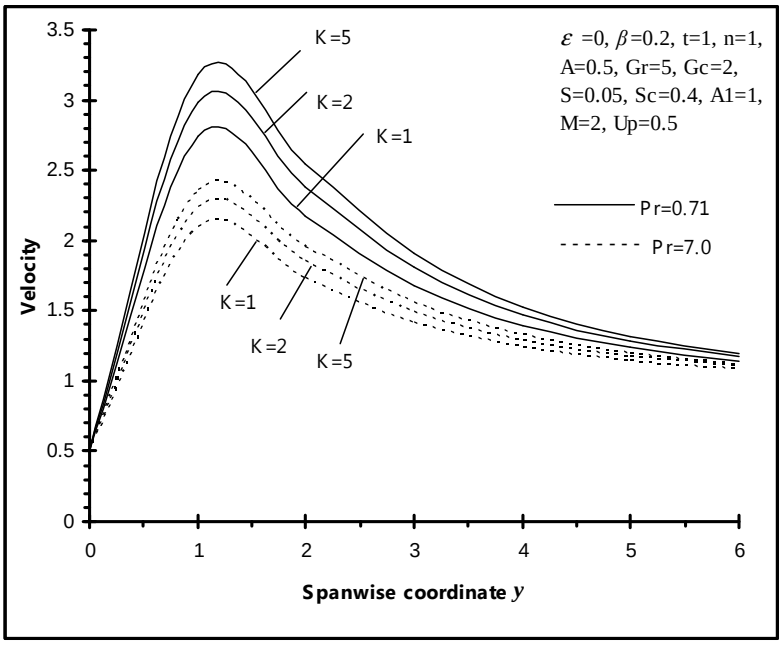

Fig.7. Velocity profiles against spanwise coordinate *y* for different values of permeability parameter *K*

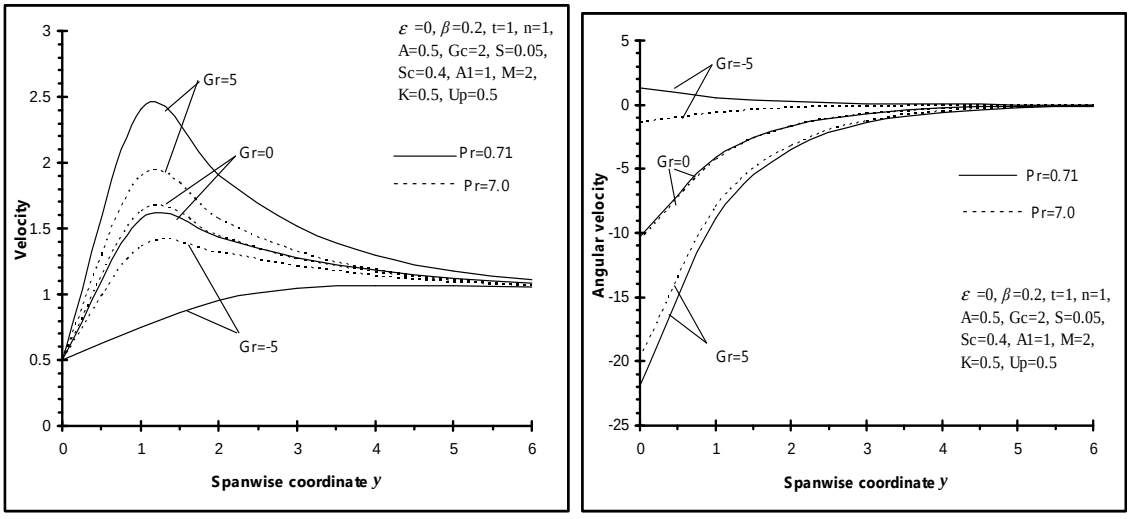

Fig.8 (a) **Fig.8 (b)**

Fig.8. Velocity and angular velocity profiles against spanwise coordinate *y* for different values of Grashof number *Gr*

The velocity profiles for different values of the permeability parameter *K* are plotted in Fig. 7. It is clear that the velocity increases due to increasing values of permeability parameter *K* both in air and water. Further, the velocity decreases with increasing Prandtl number which indicates that the velocity increases in air compared with water.

For different values of the Grashof number G_r, the velocity and angular velocity profiles are depicted in Fig. 8. It is obvious that an increase in G_r leads to a rise in the values of velocity, but decreases due to angular velocity. Negative values of G_r, which indicates the heating of the plate,

are also taken into account. Also, the large values of M and G_r respectively correspond to a strong magnetic field and to a cooling problem that is generally encountered in nuclear engineering in connection with the cooling of reactors. For G_r, the velocity decreases and angular velocity increases in water while for G_r < or = 0, the velocity decreases and angular velocity increases in air.

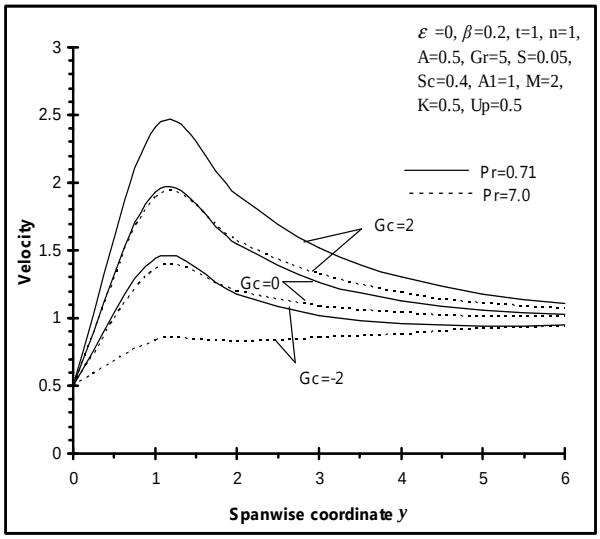

Fig.9 (a)

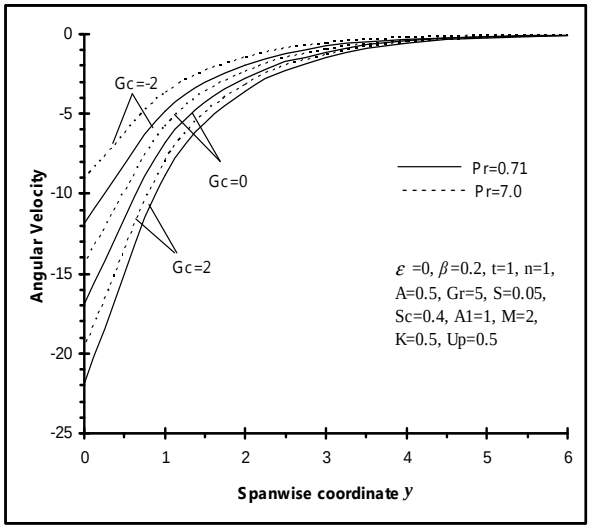

Fig.9 (b)

Fig.9. Velocity and angular velocity profiles against spanwise coordinate *y* for different values of modified Grashof number *Gc*

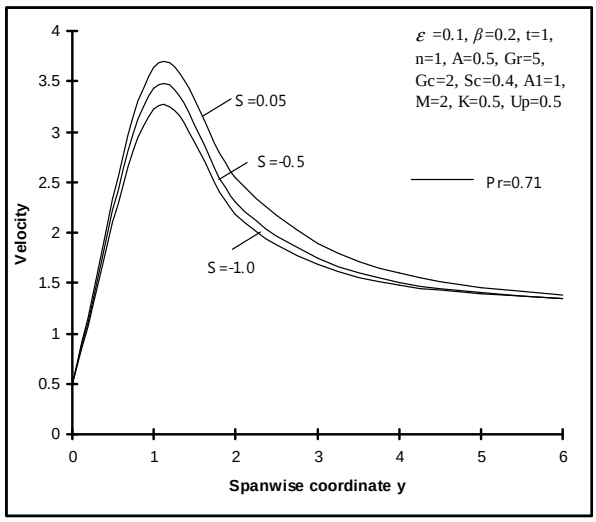

Fig.10 (a)

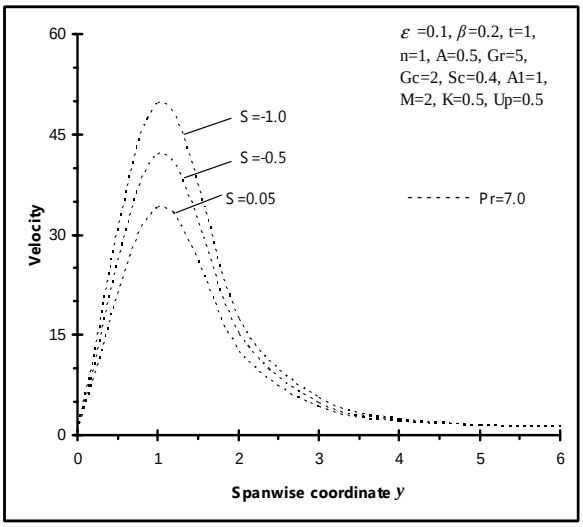

Fig.10 (b)

Fig.10. Velocity profiles against spanwise coordinate *y* for different values of source parameter *S*

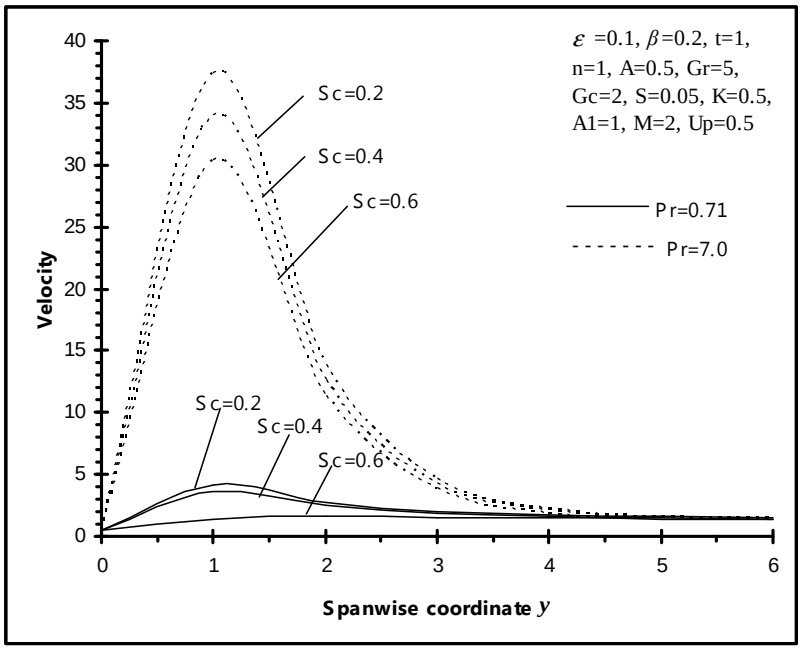

Fig.11. Velocity profiles against spanwise coordinate *y* for different values of Schmidt number *Sc*

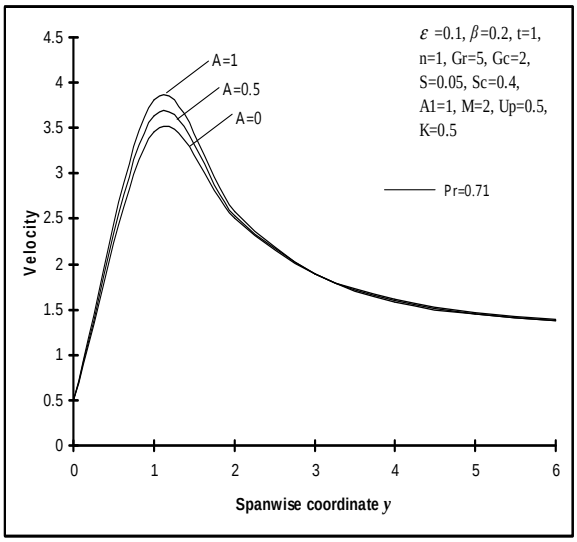

Fig.12 (a)

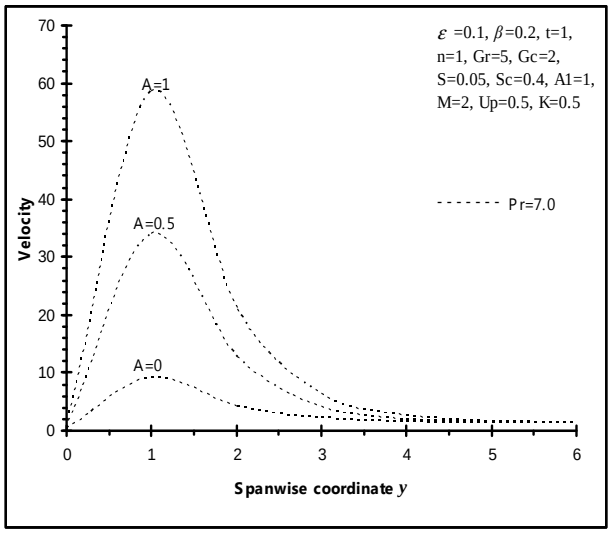

Fig.12 (b)

Fig.12. Velocity profiles against spanwise coordinate *y* for different values of suction velocity parameter *A*

Fig. 10 demonstrates the velocity profiles against spanwise coordinate *y* for various values of source parameter *S*. Clearly as *S* increases, the velocity increases in air and decreases in water. Further, the curves show that the peak value of velocity increases rapidly near the wall of the porous plate, and then decays to the free stream velocity. It is also observed that for different values of *S*, the values of velocity are increased in water compared with air.

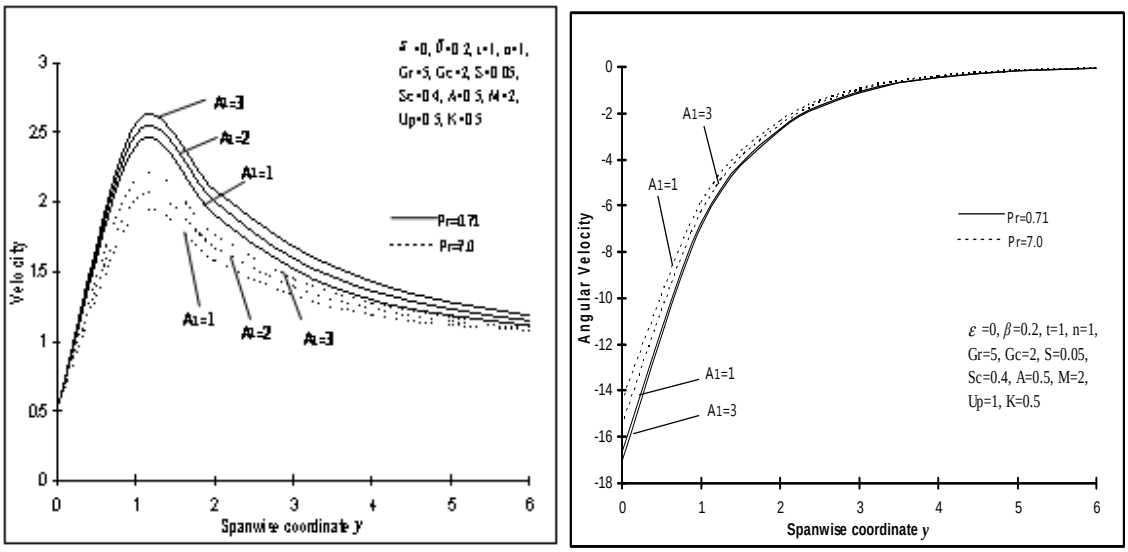

Fig.13 (a) **Fig.13 (b)**

Fig.13. Velocity and angular velocity profiles against spanwise coordinate *y* for different values of thermal diffusion parameter A_1

The velocity profiles for different values of Schmidt number S_c are plotted in Fig. 11. For Schmidt number S_c, the value 0.6 corresponds to water vapor and represents a diffusing chemical species of most common interest in air. The numerical results show that the effect of increasing Schmidt number in air and water results in a decreasing velocity distribution across the boundary layer. The results also indicate that the effect of S_c on the velocity is more in water as compared to that in air.

Table 1 for values of skin friction

For fixed $\varepsilon = 0.1$, $\beta = 0.2$, $n = 1$, $t = 1$, $U_p = 0.5$									
A_1	K	M	G_r	G_c	S_c	S	A	τ at $P_r = 0.71$	τ at $P_r = 7.0$
0.5	0.5	1	5	2	0.4	0.05	0.5	**13.29214**	**-67.8536**
0.5	0.5	1	5.5	2	0.4	0.05	0.5	14.31581	-75.7583
0.5	0.5	1	5	2	2	0.05	0.5	15.10766	-29.7018
0.5	0.5	0	5	2	0.4	0.05	0.5	12.31711	-48.4627
1	0.5	1	5	2	0.4	0.05	0.5	12.26935	-60.7385
0.5	2	1	5	2	0.4	0.05	0.5	12.37705	-37.056
0.5	0.5	1	5	3	0.4	0.05	0.5	13.73683	-63.34
0.5	0.5	1	5	2	0.4	0	0.5	13.27936	-67.8902
0.5	0.5	1	5	2	0.4	0.05	1	14.47791	-125.359

The effect of suction velocity parameter A on the velocity is presented in Fig. 12. It is obvious that an increase in A leads to a rise in the values of velocity both in air and water. Also for any fixed value of A, the velocity increases in water compared with air.

For various values of diffusion parameter A_1, the velocity and angular velocity profiles are plotted in Fig. 13. Clearly as A_1 increases, the velocity increases and angular velocity decreases in air and water both. Furthermore, the velocity graphs are lower in water and angular velocity

graphs are lower in air which indicates that at any fixed A_1, the velocity increases in air and angular velocity increases in water.

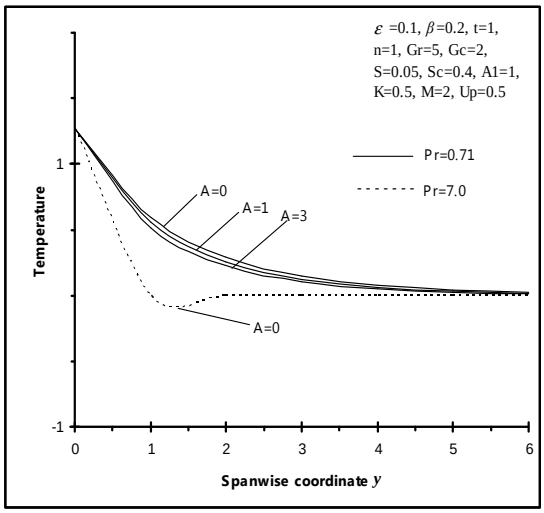

Fig.14 (a)

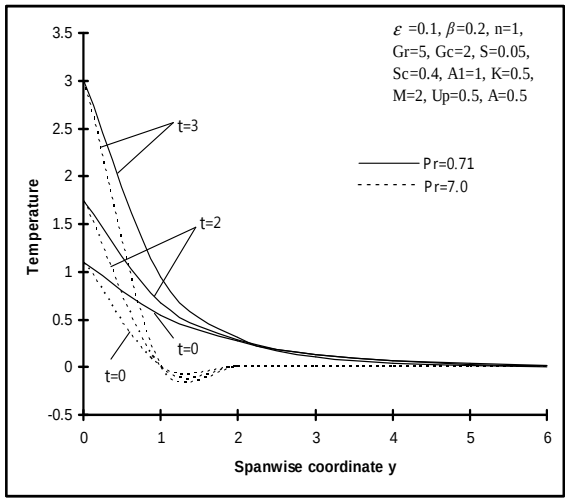

Fig.14 (b)

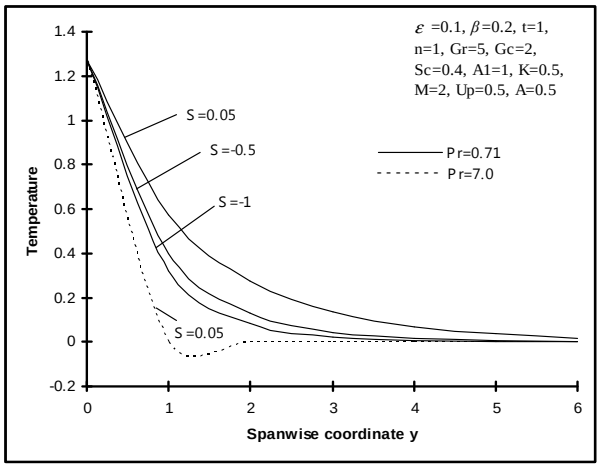

Fig.14 (c)

Fig.14. Temperature profiles against spanwise coordinate *y* for different values of suction velocity parameter *A*, dimensionless time *t* and source parameter *S*

The variations of the temperature profiles along the spanwise coordinate *y* are displayed in Fig. 14 for different values of *A*, *t* and *S* with given flow and material parameters which are listed in the figure captions. In figures 14(a), 14(b) and 14(c), it has been observed that the temperature profiles are lower in water as compared to that in air. The reason is that smaller values of P_r are equivalent to increasing thermal conductivities, and therefore heat is able to diffuse away from the heated surface more rapidly than for higher values of P_r.

As shown in Fig. 14(a), it has been observed that the effect of increasing values of suction velocity parameter *A* results in a decreasing thermal boundary layer thickness approaching to zero as *y* increases. Fig. 14(b) represents the temperature profiles for various values of dimensionless time *t*. Clearly, as *t* increases the temperature increases. Also, the curves show that

the peak value of temperature in water decreases as t increases. Fig. 14(c) depicts the effect of source parameter S on the temperature. It is clear that the temperature increases as S increases.

Finally, Table 1 is made just to show the numerical values of skin friction for different values of material parameters. It is observed that an increase in Schmidt number S_c and modified Grashof number G_c leads to a rise in the skin friction and decrease in the source parameter S leads to fall in the skin friction. Also, the skin friction decreases in air and increases in water due to increasing values of diffusion parameter A_1 and porosity parameter K. Moreover, the effect of increasing values of Grashof number G_r and suction velocity parameter A results in the increasing skin friction in air and decreasing skin friction in water. Further, in the absence of magnetic field, the skin friction decreases in air and increases in water. The results also reveal that the skin friction decreases due to increasing Prandtl number which indicates that the skin friction is more in air as compared to that in water.

CONCLUSION

The aim of this paper is to study the unsteady MHD heat and mass transfer free convection flow of an incompressible, viscous, electrically conducting polar fluid past a semi-infinite porous moving plate whose velocity is maintained at a constant value, and embedded in a porous medium subjected to the presence of a transverse magnetic field with heat source and thermal diffusion. The method of solution can be applied for small perturbation approximation. Numerical results are displayed in graphical and tabular form to illustrate the variation of velocity, angular velocity, temperature and skin friction with various governing parameters entering into the problem. The fluids taken in this study are air and water. The following conclusions are set out:

- In the absence of magnetic field, the velocity and temperature decrease in water compared with air.
- The velocity distribution is lower for a Newtonian fluid as compared with a polar fluid when the viscosity ratio β is less than 0.5.
- The angular velocity increases as the plate velocity U_p increases both in air and water.
- The velocity increases with increasing values of permeability parameter K both in air and water.
- In case of cooling of the plate $G_r > 0$, the velocity decreases and angular velocity increases in water. In case of heating of the plate $G_r < 0$, the velocity decreases and angular velocity increases in air.
- As source parameter S increases, the velocity increases in air and decreases in water.
- In air and water both, the velocity increases and angular velocity decreases due to increasing values of diffusion parameter A_1.
- The temperature increases as source parameter S increases.
- The skin friction is more in air as compared to that in water.

REFERENCES

[1] V.M. Soundalgekar, H.S. Takhar, *AIAA. J.*, 15 **(1977)**, 457-458.

[2] D.A. Nield, A. Bejan, *Convection in porous media*, 2nd edition, Springer-Verlag, Berlin **(1998)**.
[3] J.A. Shercliff, *A text book of magnetohydrodynamics*, Pergamon press, London **(1965)**.
[4] V.C.A. Ferraro, C. Plumpton, *An introduction to magneto fluid mechanics*, Claranden press, Oxford **(1966)**.
[5] K.P. Cramer, S.L. Pai, *Magneto fluid dynamics for engineers and applied physics*, Mc-Graw Hill Book Company, New York **(1973)**.
[6] E.L. Aero, A.N. Bulygin, E.V. Kuvshinskii, *J. Appl. Math. Mech.*, 29(2) **(1965)**, 333-346.
[7] N.V. Dep, *J. Appl. Math. Mech.*, 32(4) **(1968)**, 777-783.
[8] G. Lukaszewicz, *Micropolar Fluids - Theory and Applications*, Birkhauser, Boston, **1999**.
[9] A.C. Eringen, *J. Math. Mech.*, 16 **(1966)**, 1-18.
[10] A.C. Eringen, *J. Math. Anal. Appl.*, 38 **(1972)**, 480-496.
[11] I.A. Hassanien, A. Shamardan, N.M. Moursy, R.S.R. Gorla, *Int. J. Numer. Methods Heat Fluid flow*, 9 **(1999)**, 643-659.
[12] H.S. Takhar, O.A. Beg, *Int. J. Engg. Res.*, 21 **(1997)**, 87-100.
[13] M. Kumari, *Int. J. Engg. Sci.*, 36 (3) **(1998)**, 299-314.
[14] S. Sreekanth, R. Saravana, S. Venkataramana, R. Hemadri Reddy, *Advances in Appl. Sc. Research*, 2(3) **(2011)**, 246-264
[15] R.J. Gribben, *Proc. R. Soc. London*, A 287 **(1965)**, 123-141.
[16] H.S. Takhar, P.C. Ram, *Astrophys. Space Sci.*, 183 **(1991)**, 193-198.
[17] H.S. Takhar, P.C. Ram, *Int. Comm. Heat Mass Transfer*, 21 **(1994)**, 371-376.
[18] V.M. Soundalgekar, *Proc. R. Soc. London*, A 333 **(1973)**, 25-36.
[19] A.A. Raptis, N. Kafousias, *Int. J. Energy Res.*, 6 **(1982)**, 241-245.
[20] A.A. Raptis, *Int. J. Energy Res.*, 10 **(1986)**, 97-100.
[21] T.J. Cowling, *Magnetohydrodynamics*, Interscience Publishers, New York, **1957**.
[22] K. Yamamoto, N. Iwamura, *J. Eng. Math.*, 10 **(1976)**, 41-54.
[23] M.A. Samad, M. Mohebujjaman, *Res. J. of Appl. Sc., Engg. and Technology*, 1(3) **(2009)**, 98-106.
[24] R. Saravana, S. Sreekanth, S. Sreenadh, R. Hemadri Reddy, *Advances in Appl. Sc. Research*, 2(1) **(2011)**, 221-229
[25] A.K. Singh, *J. Energy Heat Mass Transfer*, 23 **(2001)**, 167-178.
[26] Youn J. Kim, *Int. J. Heat and Mass Transfer*, 44 **(2001)**, 2791-2799.
[27] Youn J. Kim, *Int. J. Engg. Sc.*, 38 **(2000)**, 833.
[28] A. Kavitha, R. Hemadri Reddy, S. Sreenadh, R. Saravana, A.N.S. Srinivas, *Advances in Appl. Sc. Research*, 2(1) **(2011)**, 269-279